The Journal of Neuroscience, September 1, 1997, 17(17):6639–6646

Prolonged Sodium Channel Inactivation Contributes to Dendritic Action Potential Attenuation in Hippocampal Pyramidal Neurons

Hae-Yoon Jung, Timothy Mickus, and Nelson Spruston

Department of Neurobiology and Physiology, Institute for Neuroscience, Northwestern University, Evanston, Illinois 60208-3520

During low-frequency firing, action potentials actively invade the dendrites of CA1 pyramidal neurons. At higher firing rates, however, activity-dependent processes result in the attenuation of back-propagating action potentials, and propagation failures occur at some dendritic branch points. We tested two major hypotheses related to this activity-dependent attenuation of back-propagating action potentials: (1) that it is mediated by a prolonged form of sodium channel inactivation and (2) that it is mediated by a persistent dendritic shunt activated by back-propagating action potentials. We found no evidence for a persistent shunt, but we did find that cumulative, prolonged inactivation of sodium channels develops during repetitive action potential firing. This inactivation is significant after a single action potential and continues to develop during several action potentials thereafter, until a steady-state sodium current is established. Recovery from this form of inactivation is much slower than its induction, but recovery can be accelerated by hyperpolarization. The similarity of these properties to the time and voltage dependence of attenuation and recovery of dendritic action potentials suggests that dendritic sodium channel inactivation contributes to the activity dependence of action potential back-propagation in CA1 neurons. Hence, the biophysical properties of dendritic sodium channels will be important determinants of action potential-mediated effects on synaptic integration and plasticity in hippocampal neurons.

Key words: dendrite; action potential; sodium channels; synaptic integration; pyramidal neuron; activity dependent

Recent experiments using simultaneous somatic and dendritic patch-pipette recordings have shown that action potentials are normally initiated in the axon and back-propagate into the dendrites of many types of CNS neurons (for review, see Stuart et al., 1997). These back-propagating action potentials are likely to provide an important spatial signal that influences ongoing synaptic integration and allows for postsynaptic firing in the axon to be associated with presynaptic activity. For example, the induction of activity-dependent changes in synaptic strength such as long-term potentiation (LTP) and long-term depression depend critically on the timing of pre- and postsynaptic inputs (Levy and Steward, 1983; Markram et al., 1997), and one form of LTP has been shown to be blocked by preventing action potentials from back-propagating into the dendrites of hippocampal pyramidal neurons (Magee and Johnston, 1997). These findings demonstrate the importance of understanding the factors that determine the extent and pattern of action potential back-propagation in pyramidal neuron dendrites.

Action potential back-propagation in CA1 dendrites is complex. At low frequencies action potentials invade most of the dendritic tree in an active fashion, whereas at higher frequencies action potentials attenuate more and may fail to actively propagate into much of the dendritic tree (Callaway and Ross, 1995; Spruston et al., 1995). The degree of action potential attenuation observed during a train of action potentials depends on the location of the recording in the dendritic tree, the number of action potentials, and the rate of firing. In distal dendrites, dramatic attenuation of action potential amplitude typically occurs after one or a few action potentials at 20 Hz, and apparent failures of active propagation are often observed at branch points, whereas attenuation is smaller and more gradual in proximal dendrites. The degree of dendritic action potential attenuation is also known to be dependent on the membrane potential between action potentials (Spruston et al., 1995), suggesting that the states of dendritic voltage-gated channels are important determinants of how action potentials spread through the dendrites. The identity of these channels, however, and their effects on action potential back-propagation are obscure. Here we describe experiments that examine the role of voltage-gated channels in the back-propagation of action potentials into the dendrites of CA1 pyramidal neurons *in vitro*.

MATERIALS AND METHODS

Slice preparation. Hippocampal slices were prepared from the brains of 14- to 45-d-old Wistar rats, which were decapitated after halothane anesthesia. Slices were cut 300 μm thick using a vibrating tissue slicer (Campden Instruments). During the dissection and slicing procedure, brains were kept in an ice-cold physiological solution. Slices were transferred to a holding chamber containing the same physiological solution at 35–37°C for 30–45 min and subsequently at room temperature. For recording, slices were transferred individually to a chamber and perfused with physiological solution at 33–37°C.

Patch-pipette recording. Slices were visualized using infrared differential interference microscopy (Stuart et al., 1993) using a fixed-stage microscope (Zeiss Axioscop) and a Newvicon camera (Dage MTI). Patch-pipette recordings were obtained under visual control on the soma or dendrites of pyramidal neurons in the CA1 region of hippocampus. High-resistance seals (2–20 GΩ) were formed using fire-polished elec-

Received May 1, 1997; revised June 20, 1997; accepted June 23, 1997.

This manuscript was supported by National Institutes of Health Grant NS35180-01 and the Human Frontiers in Science Program. Nelson Spruston is a Sloan Fellow. We thank Nace Golding and David Ferster for discussion and comments on this manuscript, and Arnd Roth for modeling our channel gating scheme.

T.M. and H.J. contributed equally to this project.

Correspondence should be addressed to Dr. Nelson Spruston, Department of Neurobiology and Physiology, Northwestern University, 2153 N. Campus Drive, Evanston, IL 60208-3520.

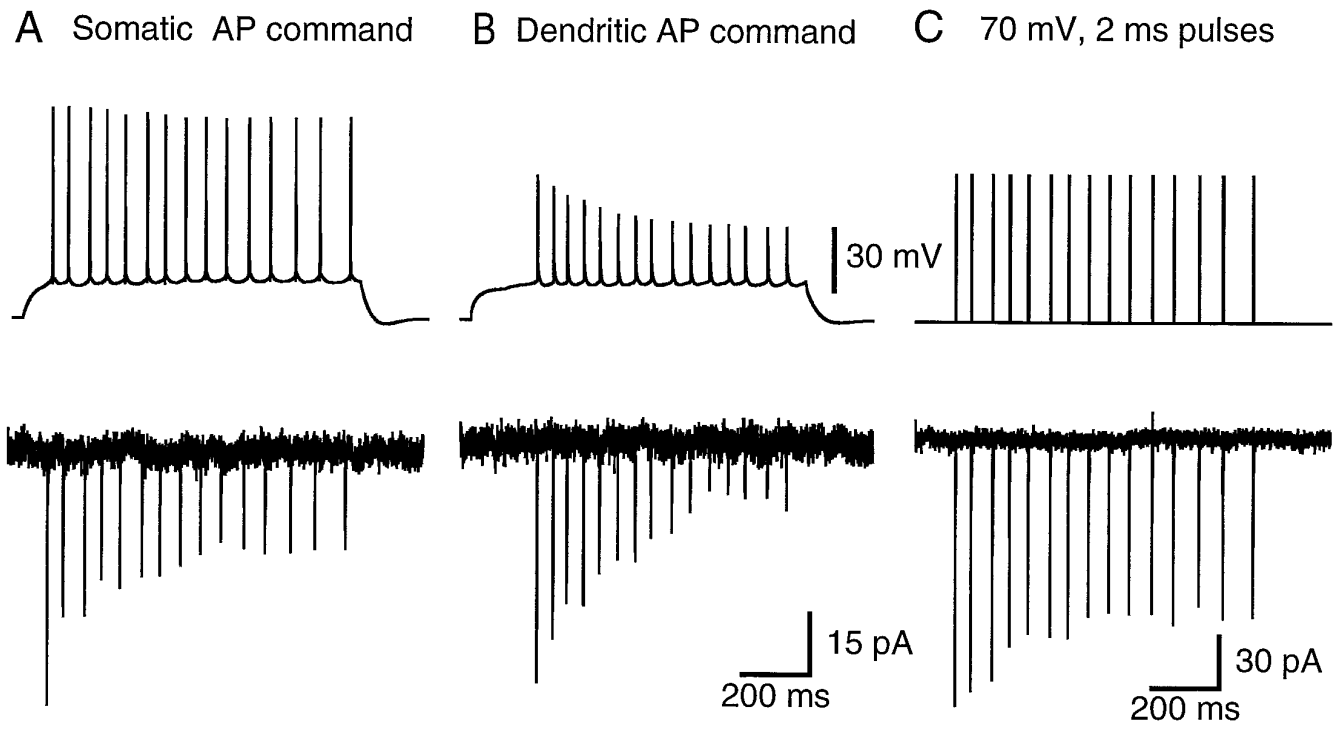

Figure 1. Cumulative, prolonged inactivation of Na^+ currents in nucleated patches. *A*, A command potential consisting of a previously recorded train of somatic action potentials evokes voltage-gated Na^+ currents in a nucleated patch. Each action potential evokes Na^+ currents that inactivate but do not fully recover during the ~50 msec interspike interval, leading to a decline in Na^+ current amplitude attributable to cumulative inactivation. *B*, A train of action potentials recorded from the apical dendrite (120 μm from the soma) of a different cell also evokes Na^+ currents exhibiting cumulative, prolonged inactivation. *C*, Cumulative, prolonged Na^+ current inactivation is also observed during repetitive depolarizations of 70 mV amplitude and 2 msec duration. Recordings in *A–C* are from the same nucleated patch and are averages of three to six trials.

trodes (thick-walled, borosilicate glass EN-1; Garner Glass Co.) pulled to tip resistances of 3–8 MΩ (Brown-Flaming P30 puller, Sutter Instrument Co.). Experiments were performed in whole-cell, cell-attached, or nucleated-patch configurations. In the whole-cell configuration, recordings were obtained in the current-clamp mode, series resistance (20–50 MΩ) was compensated with a bridge circuit, and capacitance compensation was performed. Nucleated patches were obtained by forming whole-cell recordings from somata near the surface of the slice and then withdrawing the pipette with negative pressure (0.5–1.5 psi) applied to the pipette (Sather et al., 1992). This resulted in the formation of large outside-out patches of membrane surrounding the nucleus. Whole-cell and nucleated-patch recordings were performed at 33–37°C; dendrite-attached patch recordings were performed at 27–36°C. For voltage-clamp experiments, electrodes were coated with Sylgard to reduce electrode capacitance, and the remaining patch-pipette capacitance was compensated.

Solutions and drugs. External physiological solution consisted of (in mM): 125 NaCl, 2.5 KCl, 25 $NaHCO_3$, 1.25 NaH_2PO_4, 1 $MgCl_2$, 2 $CaCl_2$, 25 dextrose. Pipette solutions for the different recording configurations were as follows (in mM): whole-cell recording: 115 potassium gluconate, 20 KCl, 10 phosphocreatine (disodium salt), 10 HEPES, 10 EGTA, 4 MgATP, 0.3 NaGTP, pH 7.3 with KOH; cell-attached recording: 120 NaCl, 3 KCl, 10 HEPES, 2 $CaCl_2$, 1 $MgCl_2$, 30 tetraethylammonium chloride (TEA), 5 4-aminopyridine (4-AP), pH 7.4 with NaOH; nucleated-patch recording: 130 CsCl, 10 phosphocreatine (disodium salt), 2 $MgCl_2$, 10 HEPES, 0.2 EGTA, 4 Na_2ATP, pH 7.4 with KOH. In some cases creatine phosphokinase (50 U/ml) was also included in the pipette solution. In most nucleated-patch experiments, 30 mM TEA and 5 mM 4-AP were added to the bath, but outward currents were negligible even in the absence of these external K^+ channel blockers. Some run-down of patch current was observed in nucleated-patch experiments. The first response in each train was monitored over time, and trials were rejected if this first response was less than two-thirds of the amplitude measured at the beginning of the experiment.

Data acquisition and analysis. Current-clamp recordings were obtained with Dagan BVC-700 amplifiers; voltage was filtered at 5 kHz and digitized at 10 kHz. Voltage-clamp recordings (nucleated- and cell-attached patches) were obtained with Axoclamp 1D and Axoclamp 200A amplifiers; current was filtered at 2 kHz and sampled at 50 kHz. Data acquisition was performed using Pulse Control software (R. Bookman, University of Miami) running under Igor Pro 3.0 (Wavemetrics) on Macintosh Power PC computers (Apple Computer) equipped with ITC-16 hardware interfaces (Instrutech Corp.). Capacitance and leak subtraction was performed by adding the current response to the test command with four responses to an inverted command potential one-fourth of the test command amplitude (i.e., −P/4 subtraction). Data analysis was performed using Igor Pro. All values are reported as mean ± SEM.

RESULTS

Action potentials recorded in the whole-cell configuration from the soma and dendrite (120 μm from the soma) of different CA1 pyramidal neurons are shown in the top traces of Figure 1*A,B*. The activity-dependent attenuation of back-propagating action potentials reported previously (Callaway and Ross, 1995; Spruston et al., 1995) is evident in this dendritic recording (Fig. 1*B*, *top trace*), obtained from a neuron maintained at 34°C in a slice from an 18-d-old rat. We tested two major hypotheses regarding the mechanisms underlying this activity-dependent action potential attenuation: (1) that attenuation is mediated by a form of Na^+ channel inactivation developing as action potentials fire and (2) that attenuation is mediated by a dendritic shunt that develops as action potentials fire.

To test the first hypothesis, Na^+ currents were examined in either cell-attached or nucleated patches (Sather et al., 1992). Inward currents were elicited by transient depolarizations using either a previously recorded train of action potentials or a series of 2–5 msec depolarizations as the command potential. These currents were mediated by TTX-sensitive Na^+ channels (see text

below) and hence are termed I_{Na}. To measure the currents during realistic depolarizations, trains of action potentials recorded from the soma or the dendrite in the whole-cell configuration (Fig. 1*A,B, top traces*) were stored and later used as command potentials to depolarize nucleated patches. This protocol allowed us to determine the nature of I_{Na} that would be flowing during normal action potential firing. The resulting patch current shows that the I_{Na} in response to repetitive action potential firing becomes progressively smaller during the train (Fig. 1*A*). When a dendritically recorded train of action potentials is used as the command in the same patch, the current attenuation is greater, as predicted because of the progressive decrease in action potential amplitude during the train (Fig. 1*B*).

Although these experiments demonstrate that I_{Na} is expected to decrease during successive action potentials in a train, the reasons for this remain unclear from this experiment. One possibility is that some Na^+ channel inactivation occurs that is slow to recover, but the slower rise of later action potentials may also contribute to the reduced I_{Na} during action potential commands. To determine whether inactivation does in fact contribute, I_{Na} was also examined in response to trains of 2–5 msec step depolarizations at 20 Hz. Figure 1*C* shows that during such a command potential, significant inactivation of I_{Na} indeed occurs. These findings support the hypothesis that Na^+ channel inactivation contributes to the attenuation of back-propagating action potentials. The first action potential leaves a fraction of dendritic Na^+ channels in the inactivated state, so the second action potential attenuates more as it propagates along the dendrite. At any dendritic location, a reduced Na^+ current flows as a result of the prolonged Na^+ channel inactivation and the smaller amplitude of the upstream action potential.

That the currents observed in experiments like those shown in Figure 1 were indeed Na^+ currents was confirmed in three nucleated-patch experiments using TTX. The currents evoked by 2 and 5 msec current pulses are shown on an expanded time scale in Figure 2. In all cases in which it was tested, 0.5 μM TTX completely blocked the currents evoked by a 20 Hz train of depolarizations ($n = 3$) (Fig. 2*A*). In response to 5 msec pulses, inactivation of I_{Na} had a time constant of 0.78 ± 0.10 msec ($n = 10$), and almost complete inactivation occurred by the end of the pulse (89 ± 3%; $n = 10$). Most experiments were performed using 2 msec depolarizations, and inactivation was almost complete during these brief depolarizations as well. At 20 Hz, however, recovery from inactivation was not complete after the 48 msec interpulse interval; on average, the amplitude of the second response was only 80% of the first response (Table 1). This remaining, prolonged form of inactivation accumulated with additional depolarizations, but complete inactivation of I_{Na} never occurred (Fig. 1*A,C*). During repetitive 20 Hz depolarizations (15–20 pulses of 50–70 mV), I_{Na} achieved a steady state that was on average 58% of the first response (Table 1). Fast inactivation appeared to be unaffected by the prolonged inactivation, because there was no significant difference between the inactivation time constants of the first and last responses in a train (paired-sample *t* test; $n = 10$; $p > 0.19$). This can be seen by the superimposition of the first response and a scaled version of the last response (Fig. 2*B,D*).

Although the inactivation of I_{Na} occurred rapidly (50% of the total inactivation was reached after the first 2 msec pulse), recovery from this form of inactivation was extremely slow, with only 72% recovery occurring after 2 sec (Fig. 3*A*, Table 1), but could be accelerated by hyperpolarization during the recovery period

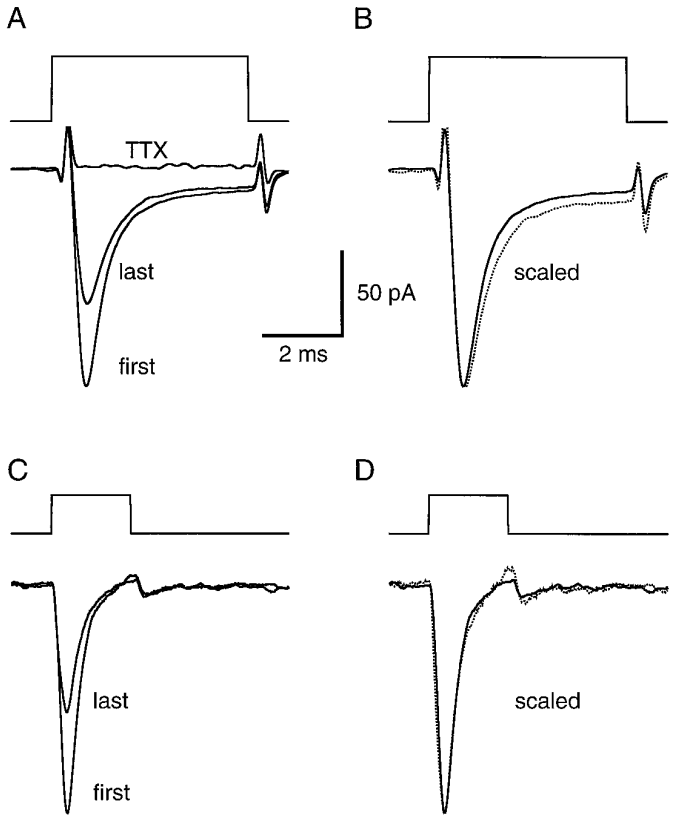

Figure 2. Na^+ currents in nucleated patches inactivate rapidly and are blocked by TTX. *A*, Voltage-gated Na^+ currents evoked by 50 mV, 5 msec depolarizations. Command potentials are shown above the current responses. The first (large) and fifteenth (small) responses in a train of step depolarizations (20 Hz) are superimposed, revealing the current reduction attributable to cumulative, prolonged inactivation. The response in the presence of 0.5 μM TTX is also superimposed. Imperfect capacitive transient subtraction is apparent at the beginning and end of the responses. Each current trace is an average of 24 trials. *B*, The same data as in *A*, but with the fifteenth response scaled (*dotted line*) to match the peak amplitude of the first response, revealing the similar time course of fast inactivation. *C*, Similar data as in *A*, but from a different nucleated patch, and in response to 50 mV, 2 msec depolarizations. Each current trace is an average of six trials. *D*, Data in *C*, with the fifteenth response scaled (*dotted line*) to match the peak amplitude of the first response.

(Fig. 3*B*). The time course and voltage dependence of the recovery from prolonged inactivation are similar to that of the recovery of back-propagating action potential amplitude (Spruston et al., 1995).

The rationale for studying the inactivation properties in nucleated patches was to take advantage of the large currents that can be obtained in this recording configuration. Because sodium channels have been shown to be similar in the soma and dendrites of CA1 pyramidal neurons (Magee and Johnston, 1995), it seems reasonable to make inferences about how the properties of somatic I_{Na} will affect action potential propagation in dendrites. To determine whether dendritic I_{Na} has the same inactivation properties as somatic I_{Na}, however, we performed experiments on I_{Na} in cell-attached dendritic patches. As expected from the relative patch size, currents in dendrite-attached patches were substantially smaller than in nucleated patches, but cumulative, prolonged inactivation of I_{Na} was still observed (Fig. 4). On average, the steady-state I_{Na} in dendritic patches was 44% of the initial current amplitude ($n = 8$; 28–240 μm from the soma) (Table 1),

Table 1. Properties of prolonged sodium channel inactivation in somatic and dendritic patches

	20 Hz Train		Recovery			
	Second pulse	Last pulse	200 msec	500 msec	1000 msec	2000 msec
% of first pulse						
Soma	80 ± 1	58 ± 2	66 ± 4	72 ± 2	77 ± 2	86 ± 4
	$n = 30$	$n = 30$	$n = 13$	$n = 17$	$n = 14$	$n = 8$
Dendrite	85 ± 2	44 ± 5	60 ± 0	63 ± 6	82 ± 1	76 ± 7
	$n = 8$	$n = 8$	$n = 2$	$n = 4$	$n = 2$	$n = 2$
% Inactivation						
Soma	20 ± 1	42 ± 2	34 ± 4	28 ± 2	23 ± 2	14 ± 4
Dendrite	15 ± 2	56 ± 5	40 ± 0	37 ± 6	18 ± 1	24 ± 7
% Recovery						
Soma			16 ± 5	33 ± 3	50 ± 3	72 ± 6
Dendrite			24 ± 1	35 ± 2	63 ± 3	61 ± 7

Statistics were calculated from peak sodium current amplitudes during 20 Hz trains of 2 msec step depolarizations and from test depolarizations at various times after the train (e.g., Figs. 1*A*, 3*A*,*B*, 4). The values of the second and last pulse responses during the train were computed as percentages of the first response (second × 100/first or last × 100/first), or as the percentage inactivation [(first − second) × 100/first or (first − last) × 100/first]. Recovery was computed as the percentage of the first response at the indicated time after the train (recovery × 100/first), as the percentage of current that remained inactivated [(first − recovery) × 100/first], or as the percent of inactivated current that had recovered [(recovery − last) × 100/(first − last)]. Values are mean ± SEM, and n is the total number of patches, which are the same for the second and third pairs as for the first pair of rows. Paired-sample t tests indicated that responses to the second and last responses were significantly smaller than the first response, for both somatic and dendritic patches ($p < 0.007$).

which was significantly greater than the attenuation observed in somatic patches (two-sample t test; $p < 0.006$). These results also obviate any concern that the prolonged inactivation of I_{Na} might be an artifact of the cytoplasmic dialysis that occurs during nucleated-patch recording.

The second hypothesis, that activity-dependent action potential back-propagation could be caused by a shunt developing in the dendrites, was tested in two ways. First, the response to a small hyperpolarizing current pulse was compared before and after a train of action potentials. Second, EPSP amplitude was compared before and after a train of action potentials. If a shunt capable of influencing action potential back-propagation develops as action potentials activate dendritic conductances, it should manifest itself as a decrease in the response to a hyperpolarizing current pulse and/or a decrease in EPSP amplitude after a train of action potentials. Furthermore, the shunt should be detectable hundreds of milliseconds after the train, when dendritic action potentials remain attenuated (Spruston et al., 1995). Figure 5 shows that no such decrease in the voltage response to a small hyperpolarizing current pulse is observed. The test response began 50 msec after the end of the depolarizing current pulse evoking the train, and the steady-state amplitude was measured 225–250 msec after the train (with the slow afterhyperpolarization subtracted) (see Fig. 5 legend). The development of a shunt would be expected to produce a significant reduction in the size of the test response. We reasoned that this change might be largest in the dendrites, where the shunt ought to develop if it were to affect action potential back-propagation, so the experiment was performed in dendritic recordings. In contrast to the prediction of a shunt, the test responses were almost identical in amplitude to the control responses (test/control = 1.01 ± 0.06 after 15–25 action potentials; $n = 7$ dendritic recordings 56–210 μm from the soma). One complicating factor in the interpretation of this experiment is the sag in the voltage response, mediated by the hyperpolarization-activated conductance I_h. An increase in this conductance (e.g., after Ca^{2+} elevation during the train) (Hagiwara and Irisawa, 1989) could produce a shunt that is masked by its own tendency to reduce the steady-state response to a hyperpolarizing current pulse. To test this possibility, we also monitored hyperpolarizing responses before and after a train in the presence of 5 mM CsCl to block I_h. Under these conditions we still found no evidence for a shunt (test/control = 0.98 ± 0.04 after 15–35 action potentials; $n = 3$ dendritic recordings 56–196 μm from the soma; data not shown).

The prediction that a dendritic shunt would produce a reduction of EPSP amplitude was also tested experimentally. EPSPs were evoked by stimulation in distal stratum radiatum or in stratum lacunosum/moleculare and monitored in somatic recordings. This experiment should maximize the likelihood of detecting a shunt, by virtue of the fact that EPSPs generated in the distal apical dendrites must travel a long distance to the soma and could be affected by a shunt anywhere along the way. Nevertheless, we found no evidence for a shunt. EPSPs varied in amplitude from trial to trial; in some cases the test EPSP was larger than control and in some cases it was smaller, but the average change in EPSP amplitude was insignificant (Fig. 6*A*) (test/control = 1.06 ± 0.05; $n = 6$). To ensure that the amplitude of the test EPSP was not affected by paired-pulse facilitation or depression independent of the train of action potentials, control experiments were performed with only a subthreshold depolarization between the two synaptic responses (Fig. 6*B*). In these experiments the control and test EPSP amplitudes were also similar (test/control = 1.06 ± 0.07; $n = 6$). The test/control EPSP ratio observed with a train of action potentials was not significantly different from the ratio with a subthreshold depolarization (paired-sample t test; $n = 6$; $p > 0.9$), suggesting that the train of action potentials does not produce a global dendritic shunt.

Two other possible mechanisms underlying activity-dependent attenuation of back-propagating action potentials were also tested: (1) that attenuation is related to voltage-gated Ca^{2+} current inactivation and (2) that attenuation is caused by a shunt induced by recurrent synaptic activation. These mechanisms we regarded as unlikely albeit formal possibilities. Both hypotheses can be excluded by the experiment shown in Figure 7. Application of $CdCl_2$ at a concentration sufficient to block high-threshold Ca^{2+} channels (200 μM) did not prevent action potential attenuation in dendritic recordings ($n = 6$). In one recording, 50 μM $NiCl_2$ was coapplied to block low-threshold Ca^{2+} channels as well, and still

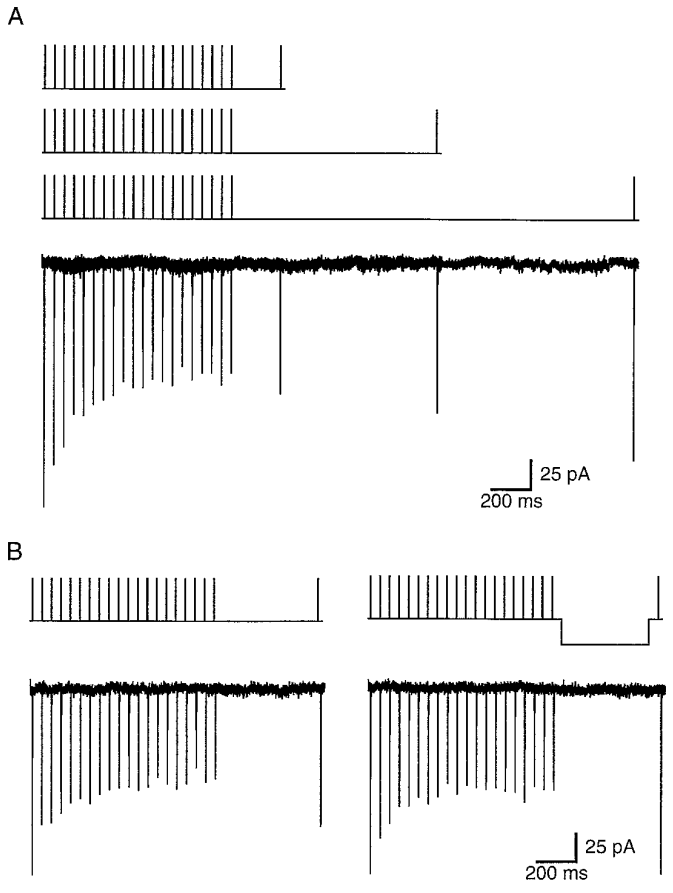

Figure 3. Na^+ current recovers slowly but is accelerated by hyperpolarization. *A*, Na^+ currents in a nucleated patch (three superimposed responses, below the three command potentials) recover very slowly from cumulative, prolonged inactivation. Test responses 200, 1000, and 2000 msec after the initial 20 Hz train of 50 mV, 2 msec depolarizations exhibit 20, 40, and 65% recovery, respectively, of the inactivated portion of the current. Each current trace is an average of three to four trials. *B*, In a different nucleated patch, recovery is accelerated by a 30 mV hyperpolarization during the 500 msec recovery period. Recovery is 49% in control (*left*) and 96% with hyperpolarization (*right*). Each current trace is an average of three trials.

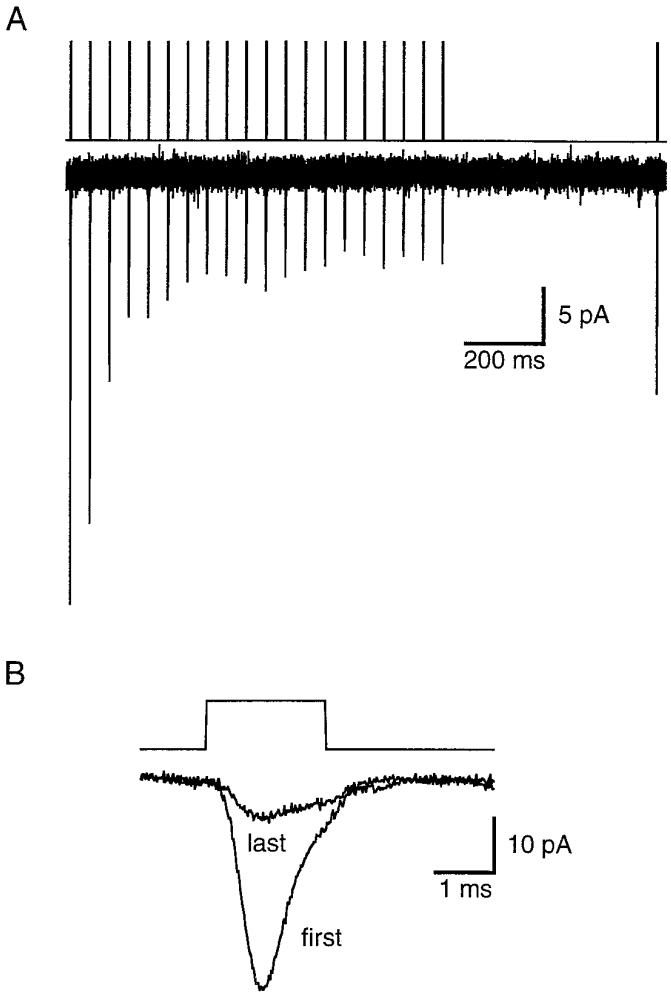

Figure 4. Na^+ currents in dendrite-attached patches also exhibit cumulative, prolonged inactivation. *A*, Na^+ currents in a dendrite-attached patch (203 μm from the soma) evoked by a 20 Hz train of 50 mV, 2 msec depolarizations. Steady-state current is 20% of the first response and 38% of the inactivated current recovered after 500 msec. The current trace is an average of 13 trials. Recording was performed at 35°C. *B*, The first and last responses in the train shown in *A* are superimposed and displayed on an expanded time scale.

no effect was observed on action potential attenuation (Fig. 7). Although the firing pattern sometimes changed slightly in the presence of these blockers (perhaps because of effects on Ca^{2+}-activated K^+ channels), activity-dependent back-propagation always persisted, indicating that neither high-threshold voltage-gated Ca^{2+} channels nor Ca^{2+}-activated K^+ channels are required for activity-induced changes in the ability of action potentials to invade CA1 dendrites. Blocking Ca^{2+} channels also completely blocked synaptic transmission (Fig. 7), thereby ruling out the possibility that action potential attenuation is mediated by recurrent synaptic activity (e.g., attributable to a shunt induced by recurrent inhibition). Similar observations were made using blockers of synaptic transmission, such as D-AP5, CNQX, and bicuculline ($n = 4$).

DISCUSSION

Our results suggest that the activity-dependent attenuation of action potentials that occurs as spikes back-propagate into the dendrites of CA1 pyramidal neurons is mediated by a cumulative, prolonged form of Na^+ channel inactivation. Action potentials are initiated in the axon of CA1 cells, probably in the first node of Ranvier (Colbert and Johnston, 1996a). Initiation is likely to occur at this site because of a high density of Na^+ channels there compared with the somatic and dendritic membrane (Mainen et al., 1995; Rapp et al., 1996). As action potentials invade the soma and dendrites, they encounter a lower density of Na^+ channels, which is sufficient to support active back-propagation, but with significant attenuation of action potential amplitude as a function of distance from the soma (Spruston et al., 1995). The data presented here indicate that as the first action potential in a train invades the dendrites, a fraction of the dendritic Na^+ channels becomes inactivated. At typical firing rates for CA1 pyramidal neurons (e.g., 20 Hz), the interspike interval is too short for complete recovery to occur from the prolonged form of inactivation, so the next spike will encounter an even lower density of available Na^+ channels, and hence this spike will attenuate more than the first spike as it propagates along the dendrite. Axonal action potentials are unlikely to be affected by prolonged Na^+ channel inactivation, however, because it is never complete, and

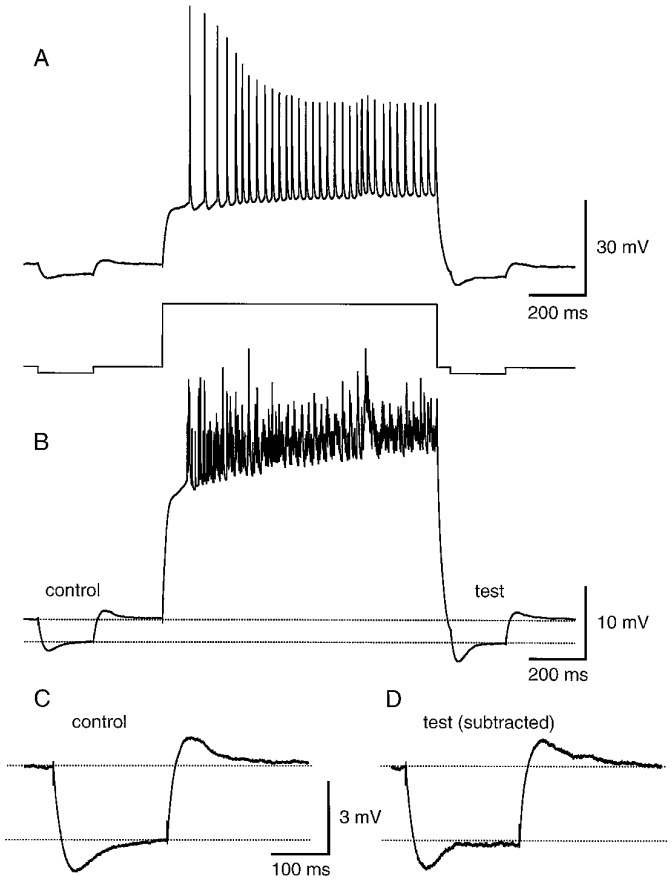

Figure 5. Small hyperpolarizing current injections in the dendrites do not reveal a global shunt after a train of action potentials. *A*, Single trace response (*top*) showing the effect of a train of 33 action potentials in 1 sec on the response to a small hyperpolarizing current pulse (*bottom*; hyperpolarizing current injections are 10 pA and depolarizing current injection is 400 pA). Apical dendritic recording is 168 μm from the soma. *B*, Average of eight responses like the one in *A*. *C*, Enlarged view of the average control hyperpolarization before the train of action potentials. *D*, Enlarged view of the average test hyperpolarization after the train of action potentials. The afterhyperpolarization measured in the absence of a test pulse was subtracted from the response with the test pulse.

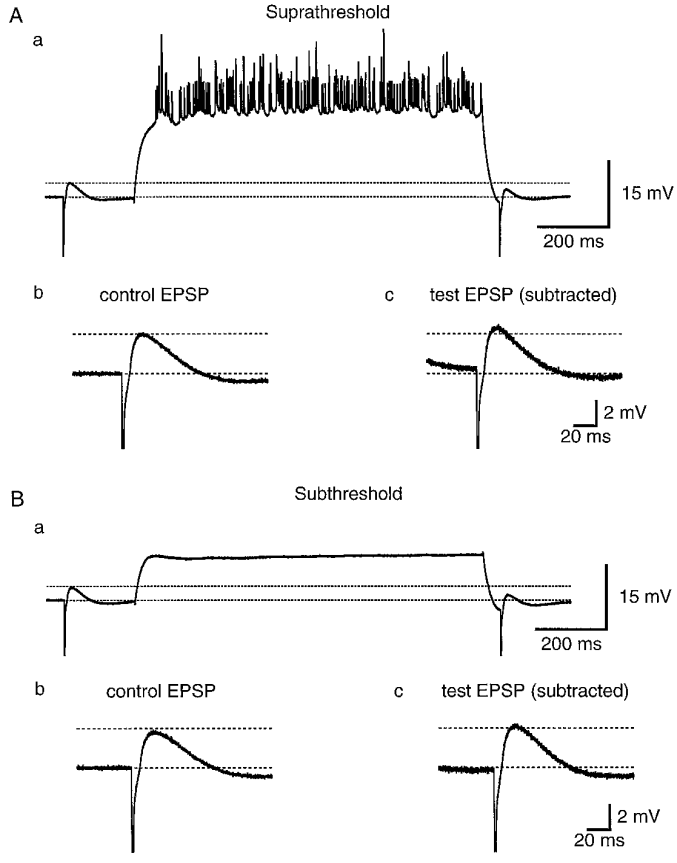

Figure 6. Somatically recorded EPSPs also do not reveal a global shunt after a train of action potentials. *A*, Average of 12 EPSPs before and after +180 pA current injections evoking trains of 16 action potentials on average (*a*). The control EPSP (*b*) and test EPSP after the train (*c*) have similar amplitudes. The afterhyperpolarization measured in the absence of a test EPSP has been subtracted from the test EPSP (*c*). *B*, Average of 11 EPSPs before and after subthreshold depolarizations evoked by a +120 pA current pulse (*a*). The control EPSP (*b*) and test EPSP (*c*) have amplitudes similar to one another and to those shown in *A*. The *dashed lines* are drawn at the same levels (relative to baseline) in *A* and *B*.

the density of Na^+ channels in the axon is likely to be so high that it is not significantly affected by the ~40% inactivation at steady state.

"Slow" inactivation of Na^+ channels has been described previously in several neuronal preparations (Narahashi, 1964; Adelman and Palti, 1969; Chandler and Meves, 1970; Schauf et al., 1976; Rudy, 1978, 1981; Belluzi and Sacchi, 1986; Ogata et al., 1990; Ruben et al., 1992; Colbert and Johnston, 1996b; Fleidervish et al., 1996). In some cases the rates of both inactivation and recovery are comparably slow, whereas in other cases, as we describe here, entry into the slow inactivated state is faster than recovery from this state. Slow inactivation has been proposed to account for slow adaptation of action potential firing in *Myxicola* axons (Rudy, 1981) and in neocortical pyramidal neurons (Fleidervish et al., 1996). This adaptation requires inactivation of sodium currents after several seconds of depolarization, whereas the molecular mechanism underlying activity-dependent action potential back-propagation must occur more rapidly, because back-propagating action potential failure can occur after even a single action potential (Spruston et al., 1995). The inactivation we describe here has this important property, and we therefore refer to this inactivation as "prolonged" rather than "slow." It is nevertheless possible that the rapidly induced yet prolonged inactivation we describe here is functionally similar to the slow inactivation described by others. For example, although Fleidervish and colleagues (1996) found that 200 msec depolarizations produced an amount of inactivation similar to what we observed with only 2 msec depolarizations, Rudy reports that in *Myxicola* axons, long depolarizations are no more effective than much shorter depolarizations at producing slow inactivation, presumably because the slow inactivated state is primarily entered from the open state (Rudy, 1981). In agreement with our data, Rudy showed that sodium channels accumulate in the slow inactivated state only if repetitive depolarizations are applied (Rudy, 1981).

Our data suggest some interesting gating properties of Na^+ channels in CA1 neurons. A gating scheme that can explain the salient features of the prolonged inactivation we describe is presented in Figure 8. The model has four states: closed (*C*), open (*O*), inactivated (*I*), and prolonged inactivated (*PI*). In developing the model, we focused on the observation that cumulative inactivation of I_{Na} occurs rapidly and reaches a substantial steady state during repetitive brief depolarizations (Figs. 1, 3, 4),

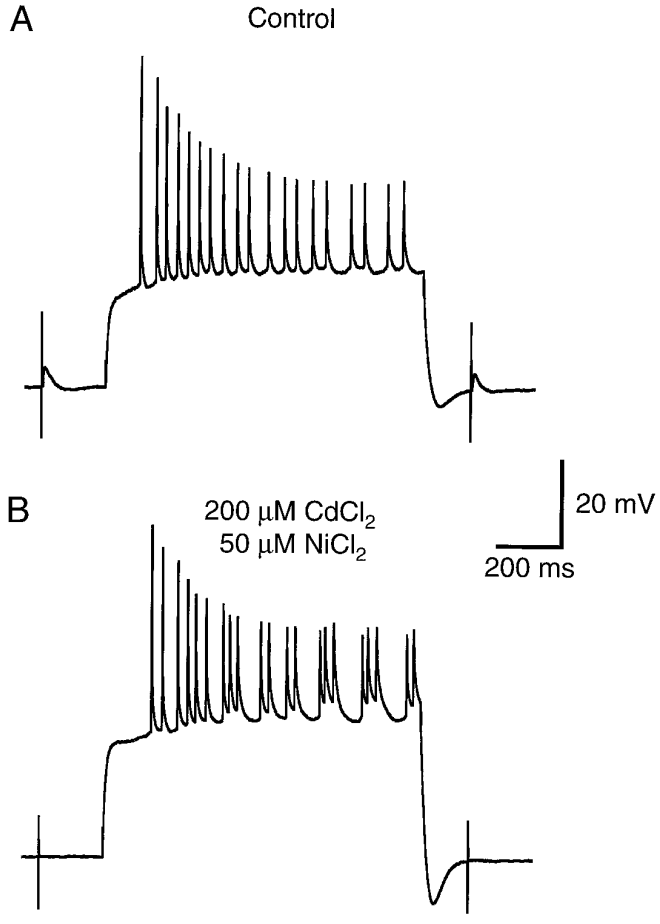

Figure 7. Blocking voltage-gated Ca^{2+} channels with $CdCl_2$ and $NiCl_2$ does not prevent activity-dependent spike attenuation in dendrites. *A*, Action potentials evoked by a +400 pA current injection in an apical dendritic recording 174 μm from the soma exhibit activity-dependent attenuation. Synaptic responses evoked before and after the train of action potentials were used to monitor the effects of $CdCl_2$ and $NiCl_2$ in *B*. *B*, Activity-dependent action potential attenuation is not affected by the application of 200 μM $CdCl_2$ and 50 μM $NiCl_2$ to block high- and low-threshold calcium channels, respectively. The effectiveness of these blockers is indicated by the elimination of the synaptic responses before and after the train (only stimulus artifacts are visible).

despite the fact that recovery from the inactivated state is much slower than the rate at which the inactivated state is reached. These observations are surprising and require some special considerations. Simpler models, in which entry into the PI state is proportional to the number of channels that open during a pulse (i.e., the O→PI transition is prominent) and the recovery (PI→C) is proportional to the number of channels already in the PI state, predict either a smaller steady-state I_{Na} or a faster recovery from prolonged inactivation. A key feature of the gating scheme shown in Figure 8 is that the total amount of prolonged inactivation during repetitive depolarizations is limited by the fact that depolarization promotes the PI→I transition and repolarization promotes the I→C transition. The PI→I transition is therefore central to the model; without it, more Na^+ channels would accumulate in the PI state and smaller currents would be observed during repetitive depolarizations. The model also explains the acceleration of recovery by hyperpolarization, by promoting the PI→C transition. Hence, our data are consistent with a model of prolonged inactivation whereby recovery from this

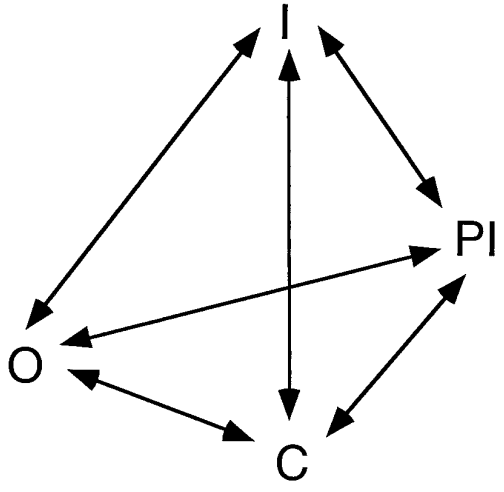

Figure 8. Model of a Na^+ channel gating scheme consistent with the properties of prolonged inactivation in hippocampal CA1 pyramidal neurons. The states are closed (*C*), open (*O*), inactivated (*I*), and prolonged inactivated (*PI*). Transitions promoted by depolarization move upward, and transitions promoted by hyperpolarization move downward. See Discussion for details.

state is promoted by both hyperpolarization *and* depolarization. Although we emphasize that this model is preliminary and cannot explain all of the available data in the literature on Na^+ channel gating, it demonstrates some interesting features that more complete models should take into account.

An alternative to such a complex gating scheme, however, is that multiple populations of channels may exist, some that undergo prolonged inactivation and others that do not. Such distinct subpopulations of Na^+ channels could arise because of different α subunits, accessory subunits, or post-translational modifications (possibly differentially distributed or susceptible to neuromodulation). Distinguishing between these possibilities will require additional experiments. Understanding whether the prolonged inactivation properties of I_{Na} are determined by one population or multiple populations of Na^+ channels will also help to elucidate the mechanisms underlying the difference in the prolonged inactivation of somatic and dendritic I_{Na}. One possibility is that the increased prolonged inactivation of dendritic I_{Na} is caused by differential post-translational modification of the same gene product found at the soma; alternatively, multiple gene products could be differentially distributed along the somato-dendritic axis.

Prolonged Na^+ channel inactivation has been shown to produce attenuation of back-propagating action potentials in a computational model (Migliore, 1996). The degree of inactivation used in the model, however, is substantially greater than we observed, so it remains to be determined whether Na^+ channel inactivation alone is sufficient to explain all observed features of the back-propagation during trains of action potentials, including complexities such as asymmetrical branch point failures (Spruston et al., 1995). The model also showed that a dendritic shunt could be responsible for activity-dependent attenuation of back-propagating action potentials. We find no evidence for such a shunt, but a few caveats should be noted regarding this interpretation. First, the method we used relies on an ability to discern changes in input conductance as a change in the response to a hyperpolarizing current pulse or an EPSP. Although we would expect a shunt to be measurable by these methods if it is sufficient to alter the nature of spike back-propagation, we have not tested

this explicitly with a computational model. The fact that we cannot measure a shunt associated with the slow afterhyperpolarization suggests that such shunt conductances are small under our conditions, but it also indicates that the sensitivity of our method is limited. Second, a shunt could be activated at potentials reached during an action potential but could be inactive at rest; such a mechanism was included in the computational model mentioned previously (Migliore, 1996). Although this is theoretically possible, it requires a very particular biophysical mechanism (e.g., a strongly rectifying shunt conductance). Finally, we cannot rule out the possibility that small, localized shunts could affect back-propagation but might be difficult to measure in the whole cell. For example, local hot spots of voltage-gated K^+ channels could theoretically mediate asymmetrical propagation of action potentials into different regions of the dendritic tree.

Our experiments examine the question of which mechanisms are responsible for action potential back-propagation in the resting state *in vitro. In vivo*, other considerations are likely to come into play. For example, shunting and hyperpolarization attributable to inhibition have been shown to limit the back-propagation of action potentials into CA1 dendrites (Tsubokawa and Ross, 1996). This may provide a mechanism for selectively allowing back-propagating action potentials to reach certain dendritic compartments, but not others, under defined conditions of interneuron activity. Such a mechanism might function to selectively promote or inhibit associative plasticity in restricted sets of synaptic inputs onto CA1 dendrites. Determining how spike back-propagation might be regulated by inhibition or neuromodulation of Na^+ channel inactivation will be an important direction for future studies aimed at understanding the complex process of synaptic integration in these and other neurons.

REFERENCES

Adelman WJ, Palti Y (1969) The effects of external potassium and long duration voltage conditioning on the amplitude of sodium currents in the giant axon of the squid, *Loligo pealei*. J Gen Physiol 54:589–606.

Belluzi O, Sacchi O (1986) A quantitative description of the sodium current in the rat sympathetic neurone. J Physiol (Lond) 380:275–291.

Callaway JC, Ross WN (1995) Frequency-dependent propagation of sodium action potentials in dendrites of hippocampal CA1 pyramidal neurons. J Neurophysiol 74:1395–1403.

Chandler WK, Meves H (1970) Slow changes in membrane permeability and long-lasting action potentials in axons perfused with fluoride solutions. J Physiol (Lond) 211:707–728.

Colbert CM, Johnston D (1996a) Axonal action-potential initiation and Na^+ channel densities in the soma and axon initial segment of subicular pyramidal neurons. J Neurosci 16:6676–6686.

Colbert CM, Johnston D (1996b) A decrease in Na^+ current contributes to loss of action potential amplitude in dendritic spike trains. Soc Neurosci Abstr 22:791.

Fleidervish IA, Friedman A, Gutnick MJ (1996) Slow inactivation of Na+ current and slow cumulative spike adaptation in mouse and guinea pig neocortical neurones in slices. J Physiol (Lond) 493:83–97.

Hagiwara N, Irisawa H (1989) Modulation by intracellular Ca^{2+} of the hyperpolarization activated inward current in rabbit single sino-atrial node cells. J Physiol (Lond) 409:121–141.

Levy WB, Steward O (1983) Temporal contiguity requirements for long-term associative potentiation/depression in the hippocampus. Neuroscience 8:791–797.

Magee JC, Johnston D (1995) Characterization of single voltage-gated Na^+ and Ca^{2+} channels in apical dendrites of rat CA1 pyramidal neurons. J Physiol (Lond) 487:67–90.

Magee JC, Johnston D (1997) A synaptically controlled, associative signal for Hebbian plasticity in hippocampal neurons. Science 275:209–213.

Mainen ZF, Joerges J, Huguenard JR, Sejnowski TJ (1995) A model of spike initiation in neocortical pyramidal neurons. Neuron 15:1427–1439.

Markram H, Lübke J, Frotscher M, Sakmann B (1997) Regulation of synaptic efficacy by coincidence of postsynaptic APs and EPSPs. Science 275:213–215.

Migliore M (1996) Modeling the attenuation and failure of action potentials in the dendrites of hippocampal neurons. Biophys J 71:2394–2403.

Narahashi T (1964) Restoration of action potential by anodal polarization in lobster giant axons. J Cell Comp Physiol 64:73–96.

Ogata N, Yoshii M, Narahashi T (1990) Differential block of sodium and calcium channels by chlorpromazine in mouse neuroblastoma cells. J Physiol (Lond) 420:165–183.

Rapp M, Yarom M, Segev I (1996) Modeling back propagating action potentials in weakly excitable dendrites of neocortical pyramidal cells. Proc Natl Acad Sci USA 93:11985–11990.

Ruben PC, Starkus JG, Rayner MD (1992) Steady-state availability of sodium channels: interactions between activation and slow inactivation. Biophys J 61:941–955.

Rudy B (1978) Slow inactivation of the sodium conductance in squid giant axons. Pronase resistance. J Physiol (Lond) 283:1–21.

Rudy B (1981) Inactivation in *Myxicola* giant axons responsible for slow and accumulative adaptation phenomena. J Physiol (Lond) 312:531–549.

Sather W, Dieudonné S, MacDonald JF, Ascher P (1992) Activation and desensitization of *N*-methyl-D-aspartate receptors in nucleated outside-out patches from mouse neurones. J Physiol (Lond) 450:643–672.

Schauf CL, Pencek TL, Davis FA (1976) Slow sodium inactivation in *Myxicola* axons. Biophys J 16:771–778.

Spruston N, Schiller Y, Stuart G, Sakmann B (1995) Activity-dependent action potential invasion and calcium influx into hippocampal CA1 dendrites. Science 268:297–300.

Stuart G, Spruston N, Sakmann B, Häusser M (1997) Action potential initiation and backpropagation in neurons of the mammalian CNS. Trends Neurosci 20:125–131.

Stuart GJ, Dodt H-U, Sakmann B (1993) Patch-clamp recordings from the soma and dendrites of neurons in brain slices using infrared video microscopy. Pflügers Arch 423:511–518.

Tsubokawa H, Ross WN (1996) IPSPs modulate spike backpropagation and associated $[Ca^{2+}]_i$ changes in the dendrites of hippocampal CA1 pyramidal neurons. J Neurophysiol 76:2896–2906.